Molecular Dynamics Simulation Study of Ethylene Glycol, Ethylenediamine, and 2-Aminoethanol. 2. Structure in Aqueous Solutions

A. V. Gubskaya and P. G. Kusalik*

Department of Chemistry, Dalhousie University, Halifax, Nova Scotia, B3H 4J3, Canada

Received: March 10, 2004; In Final Form: June 17, 2004

In this article, we report a molecular dynamics (MD) simulation study of the local structure in aqueous solutions of ethylene glycol (EG), ethylenediamine (ED), and 2-aminoethanol (AE), where the results are presented and discussed in a comparative manner. Four compositions (organic solute mole fractions of $X = 0.03$, 0.1, 0.3, and 0.8) were investigated for each compound. The OPLS-based potential models, as described in our companion paper [A. V. Gubskaya, P. G. Kusalik, *J. Phys. Chem.*, **2004**, *108*, XXXX] are used to represent the ethane derivatives and the SPC/E model is used for water. Thermodynamic, dynamic, and molecular structural characteristics are calculated and compared whenever possible with previous theoretical and experimental findings. The local structure in the solutions of interest is examined by means of radial and spatial distribution functions (RDFs and SDFs, respectively). The revealed three-dimensional picture of hydration confirms the presence of hydrogen-bonding arrangements that are comprised of both strong and weak hydrogen bonds, reminiscent of those found in pure liquids of EG, ED, and AE. Several interesting trends in the behavior specific to water are noted. These include a tendency for the association of water molecules in water-poor solutions, the maintenance of tetrahedral coordination in water-rich solutions, and a clear preference for hydrophilic hydration of these organic solutes at high concentrations. Despite the presence of a hydrophobic hydrocarbon backbone within the compounds studied, there is no specific tendency for hydrophobic self-association observed; however, there is some evidence of such self-association in those systems where the organic molecules adopt a *trans* ("open chain") conformation such as in ED solution. This work again clearly shows the ability of SDFs to provide detailed insights into the local structure of strongly associated molecular liquids, while, at the same time, revealing the structural complexity that results for solutions of conformationally flexible molecules.

1. Introduction

This work builds on a series of molecular dynamics (MD) investigations that have focused on the spatial solvation structure within selected strongly associated, hydrogen-bonded liquids and solutions. One of the primary tools utilized in these investigations is the application of three-dimensional atomic density maps, which are known as the spatial distribution functions (SDFs). The results obtained using this approach for water,[1] methanol,[2] water−methanol,[3] water−acetonitrile,[4−6] and water−dimethylsulfoxide (DMSO) mixtures[7] confirmed that SDFs provide a detailed and revealing picture of the solvation structure for these liquids and solutions. In the present study, the aqueous mixtures of three of the most-common representatives of 1,2-disubstituted ethanes—namely, ethylenediamine (ED, $(CH_2NH_2)_2$), 2-aminoethanol (AE, $NH_2(CH_2)_2OH$), and ethylene glycol (EG, $(CH_2OH)_2$)—are investigated. The possible presence of an intramolecular hydrogen bond between two vicinal (hydroxyl and/or amino) groups, which is a well-known feature found in isolated molecules of these three compounds, raises the following question: are the intramolecular hydrogen bonds typical in the gas phase disrupted in aqueous solution to permit additional hydrogen bonding with water molecules? A detailed structural analysis of the hydration structure of these molecules should help us to answer this question, to understand the role of cooperative effects better, as well as to provide insights into the hydration structure and behavior of larger molecules containing similar functional groups.

Methanol, as the simplest (smallest) alcohol, has served as a suitable model molecule for studies of structural aspects of solvation in nonelectrolyte aqueous mixtures. Jorgensen and Madura[8] and Laaksonen et al.[3] independently performed computer simulation studies of the hydration structure in methanol solutions, using, respectively, Monte Carlo (MC) and MD simulation techniques. Analysis of the solute−solvent radial distribution functions (RDFs) confirmed that the water molecules form a cagelike structure around the methyl group, while two or three water (H_2O) molecules are hydrogen-bonded to the hydroxyl end of the methanol.[8] These findings are in reasonable agreement with the more-recent neutron diffraction studies by Soper and Finney.[9] However, further structural details were revealed from analysis based on O−O SDFs.[3] In methanol-rich solutions, the water−water correlations were evident, even at longer range, and indicate a tendency to form chains of water molecules, whereas those for methanol resembled its pure liquid structure.[3]

Previously reported investigations of aqueous amine solutions include MC simulation studies of low-concentration water−methylamine mixtures,[10−12] a hybrid RISM-SCF study of methylamines examining their basicity anomaly in aqueous solution,[13] several simulation studies focused upon solvation free energies of simple amines,[14−16] and investigations of the solvation structure of methylamine in aqueous solutions.[17,18]

* Author to whom correspondence should be addressed. Telephone: (902) 494-3627. Fax: (902) 494-1310. E-mail address: Peter.Kusalik@dal.ca.

10.1021/jp048921+ CCC: $27.50
Published on Web 08/11/2004

Kusalik et al.[18] performed MD simulations of 10 and 30 wt % aqueous solutions of methylamine. RDFs and SDFs were used in their structural analysis. Aspects of the determined hydration structure were rather unexpected. Two primary types of hydrogen-bonded water molecules were observed. On average, two molecules are involved in making strong hydrogen bonds: one as an accepting neighbor and one as a donating neighbor. The second hydrogen-bond-forming site of the amino group is not vacant but, instead, is occupied by a more distant nearest-neighbor H_2O molecule that forms only a weak hydrogen bond to the amino hydrogen.[18] No long-range correlations of methylamine molecules were observed, as was the case in dilute methanol solution.[3]

Unfortunately, there are few computational investigations on aqueous solutions of 1,2-disubstituted ethanes. Among all representatives of this class of binary mixtures, aqueous solutions of EG have received the most research attention.[19−23] The effects of hydration on the EG molecule were studied theoretically with explicit solvent inclusion by Nagy et al.[20] and Hooft et al.[21] The OPLS force field[24] and the TIP4P water model[25] were used in the MC simulations performed by Nagy et al.,[20] whereas in the work by Hooft et al.,[21] MD methods with GROMOS force field[26] and the SPC[27] water model were utilized. The authors in refs 20 and 21 focused on four conformers (tTt, tGg′, gGg′, and g′Gg′) and considered changes in free energies when individual dihedral angles varied, thus connecting one conformer to another. Both Nagy et al.[20] and Hooft et al.[21] revealed that the tTt rotamer is better solvated than tGg′, with a free-energy difference of ∼5 kJ/mol. Assuming that there is only a single form of the *trans* conformer (tTt), Nagy et al.[20] predicted a 99:1 *gauche*:*trans* ratio in aqueous solution. In contrast, Hooft et al.,[21] taking into account all possible conformers, predicted a 67:33 *gauche*:*trans* ratio for the same equilibrium in aqueous solution. Hooft et al.[21] also concluded that the gas-phase preference for internally hydrogen-bonded solute molecules disappears completely in dilute aqueous solution.

An alternative method, in which the solvent was represented by a continuum dielectric, was used by Alagona and Ghio[22] and by Varnek et al.[23] to analyze the effects of aqueous solvation on the EG molecule. The polarized continuum model of Tomasi and co-workers[28] was used to accomplish this task. Alagona and Ghio[22] considered differences exclusively in the electrostatic contributions to the solvation free energy at the HF/4-31G and HF/6-31G* levels for the four most-stable conformers. At both of these levels, they found that the tTt rotamer is better solvated than the tGg′ rotamer by only 0.84 kJ/mol, but gGg′ and g′Gg′ are better solvated than tGg′ by 2.5−4.6 kJ/mol. Varnek et al.,[23] taking into account both the solvation and the intrinsic energy terms, reported the order of relative stabilities among *cis*, *gauche*, and *trans* conformers of EG in water. They found that the most-stable form is *gauche* (with an OCCO dihedral angle of 54°), followed by *cis* ($\Delta E = 18.8$ kJ/mol) and then *trans* ($\Delta E = 45.2$ kJ/mol).[23] Their prediction of the *gauche* form being the most stable is consistent with the results of Nagy et al.[20] with explicit water included in the simulations.

In view of the large *trans* population predicted by Hooft et al.,[21] Cramer and Truhlar[19] questioned whether this dramatic predicted solvation effect is valid. They presented a third approach for analyzing the conformational equilibrium in aqueous solutions of EG, which used quantum statistical solvation models, in particular, the Austin Model 1 (AM1-SM1a, AM1-SM2) and the Parametrized Model 3 (PM3-SM3) solvation models, which are discussed in detail in ref 19. Their results suggest that, upon passing from the gas phase into aqueous solution, there is a relative increase in the population of *trans* conformers by a factor of 3−5 (to ∼6%−10%). For example, for the relaxed SM3 model, the *gauche*:*trans* ratio is 92:8, versus 98:2 in the gas phase. This difference comes from an increase in the population of the *trans* conformers tTg and gTg′, at the expense of conformer g′Gg′.[19] Overall, these estimates for the *gauche*:*trans* ratio lie somewhere between those obtained by Nagy et al.[20] and Hooft et al.[21] and they are in close agreement with available experimental results.[29,30]

To the best of our knowledge, there have been no theoretical investigations of the local hydration structure in solutions of EG. Similarly, there have been not simulation studies probing the local structure in binary aqueous mixtures of ED or AE; moreover, there seems to be no reliable sources of information available for the conformational equilibrium in these particular molecular systems.

In the present study, MD simulations were performed for aqueous mixtures of EG, ED, and AE; four compositions of each compound were considered. The local hydration structure was analyzed by means of RDFs and SDFs to gain structural insights into the hydrogen-bonding pattern. In this publication, we will attempt to answer questions such as:

(1) How does the population of conformers change with concentration, and what is the role of hydration?

(2) Is there any specificity in how water molecules organize themselves around hydroxyl and amino groups?

(3) How is the hydration of these organic molecules influenced by a deficiency or an excess of water?

(4) How does the degree of hydration influence transport properties (i.e., diffusion constants) in the systems studied?

The paper is outlined in the following way. Section 2 describes our simulation methodology, whereas Section 3 presents results for the conformational, dynamical, and structural behavior of the systems studied, and Section 4 provides our final conclusions. Throughout this paper, the term "solute" is used with respect to the *organic* components of the aqueous mixtures.

2. Simulation Specifications

In our preceding paper,[31] we have described, in detail, the molecular and potential models used in simulations of pure liquids of EG, ED, and AE. The different model representations were tested and, on the grounds of the criteria introduced, only united-atom molecular models with rigid bonds based on the OPLS force field proposed by Jorgensen and co-workers for alcohols and amines[16,24] were selected for our simulations of pure liquids and their aqueous solutions. For each of these models, four compositions, representing various typical cases along the concentration axis, were prepared. For all compositions, EG and AE were simulated with 1−4 electrostatic and Lennard-Jones (LJ) interactions scaled by the factors of 1/1.2 (from ref 32) and 1/8 (from refs 33 and 34), respectively, whereas in the case of ED, simulations were performed without scaling of the nonbonded interactions. A compatible water model (SPC/E), devised by Berendsen et al.,[35] was chosen for balanced cross interactions between solute and solvent molecules.

The M.DynaMix simulation package[36] with truncated octahedron boundary conditions was used in the present study. The Ewald method and usual Lorentz−Berthelot combination rules were used to treat long-range electrostatic and cross interactions, respectively.[37] Bond lengths were constrained by applying the SHAKE algorithm.[38] A more-detailed description of the simulation specifications can be found in ref 31.

TABLE 1: Simulation Specifications for Aqueous Solutions of Ethylene Glycol (EG), Ethylenediamine (ED), and 2-Aminoethanol (AE) at 298 K

	run I	run II	run III	run IV
number of H_2O molecules	248	230	179	51
number of solute molecules	8	26	77	205
mole fraction of solute, X	0.03	0.1	0.3	0.8
time step (fs)	0.5	0.5	0.5	0.5
equilibration time (ns)	0.3	0.3	0.2	0.2
production time (ns)	1.4	0.7	0.3	0.8

Similar to our simulations of pure liquids, all solutions were studied at room temperature (298 K) and experimental densities.[39−41] Both canonical (NVT) and isothermal−isobaric (NPT) conditions have been utilized; the former was used consistently throughout this work. A Nosé−Hoover thermostat and barostat, with corresponding coupling parameters of 300 and 700 fs, respectively, were used to maintain temperature and pressure,[36] as required. Constant pressure conditions have been applied to selected compositions of aqueous solutions when accurate experimental densities were not available. Aqueous systems consisting of a total of 256 molecules were simulated for 1 ns, with averages collected after 200−300 ps, for most solutions studied (see Table 1 for details).

In addition to the M.DynaMix program, other computational software has been utilized in the present work. The GAUSSIAN 98[42] has been used to produce starting internal coordinates for all molecular models and visualization of the SDFs has been performed using the gOpenMol graphics software package.[43]

3. Results and Discussion

3.1. Energetic and Dynamic Properties of Binary Mixtures. Simulation results for the energies for each of the four compositions of EG, ED, and AE in water are given in Table 2 (the intermolecular energies are given per mole of solution). The average total configurational energy, $\langle U \rangle$, is comprised of the average potential energies due to solute−solute, solute−solvent, and solvent−solvent interactions and intramolecular energies. The intermolecular energies, in turn, can be divided into short-range (LJ) and long-range (Coulombic) contributions to investigate the significance of specific interactions to changes in the local structure. Table 2 shows that a 14−20-fold increase in the magnitudes of $\langle U_Q \rangle$ for the solute−solute intermolecular energies in going from dilute to concentrated solutions. This trend is most pronounced in the case of ED. The corresponding magnitudes of the solute−solute $\langle U_{LJ} \rangle$ behave in a similar fashion but increase less dramatically (by a factor of ∼8−9) for all compounds. It can also be clearly seen that the major contribution to the solute−solute intermolecular energy is electrostatic for all compounds and compositions, with the only exception being the three most dilute solutions of ED. This unusual behavior can be explained by a nonspecific association of the hydrophobic chains of the ED molecules in *trans* conformation when they are otherwise surrounded by aqueous media, as will be discussed further below.

It is also useful to examine solute−solute and water−water contributions to the total average energies normalized per molecule of that species (not shown in Table 2 but can be obtained by summation of the corresponding $\langle U_Q \rangle$ and $\langle U_{LJ} \rangle$ terms, followed by division by the respective mole fractions). The values calculated seem to be very similar in magnitude for all types of 1,2-disubstituted ethanes when the same compositions are compared. The magnitudes of solute−solute energies decrease from −128.7, −111.7, and −101.33 kJ/mol at X = 0.03 for EG, ED, and AE, respectively, to approximately −57 to −69 kJ/mol for X = 0.8. This trend reflects the apparent increase in the extent of favorable arrangements of the organic solute molecules in dilute aqueous solutions. Somewhat similar behavior was also observed in the case of water−water interactions (e.g., −49.42, −49.40, and −49.04 kJ/mol for water-rich compositions and −47.1, −41.1, and −38.5 kJ/mol for X = 0.8 of ED, AE, and EG, respectively). The fact that the present water−water energies for the water-rich solutions are larger in magnitude than the value obtained for pure SPC/E water (−47.07 kJ/mol) suggests a strengthening in water−water correlations (structure-making) in these dilute solutions, similar to that found for water−methanol mixtures.[3] Finally, a comparison of the total configurational energies reveals a consistent increase in their values (actually changing sign) from X = 0.03 to X = 0.8 for all compounds. This behavior results because of the large positive intramolecular contributions to the total energy for all ethane derivatives. In addition, we have used the total configurational energies to estimate excess energies of mixing for all mixtures and compositions studied. The resulting values (not shown) were compared with available experimental estimates of the molar excess enthalpies of mixing for AE[44] and EG[45] solutions and very good qualitative agreement was observed in both cases.

TABLE 2: Contributions to the Intermolecular Energies and the Total System Energies for Aqueous Mixtures of Ethylene Glycol (EG), Ethylenediamine (ED), and 2-Aminoethanol (AE)

	energy at composition X (kJ/mol)				maximum
system	X = 0.03	X = 0.1	X = 0.3	X = 0.8	error
EG−EG					
$\langle U_Q \rangle$	−2.44	−6.99	−19.51	−42.86	0.52
$\langle U_{LJ} \rangle$	−1.42	−4.27	−8.92	−12.11	0.02
EG−H_2O					
$\langle U_Q \rangle$	−121.64	−107.84	−75.49	−77.20	1.80
$\langle U_{LJ} \rangle$	−3.63	−0.73	3.03	8.38	0.08
H_2O−H_2O					
$\langle U_Q \rangle$	−56.50	−51.43	−37.75	−9.83	0.23
$\langle U_{LJ} \rangle$	8.93	8.57	7.08	2.14	0.03
$\langle U_{tot} \rangle$	**−43.94**	**−37.82**	**−20.25**	**24.08**	**0.02**
ED−ED					
$\langle U_Q \rangle$	−1.50	−4.22	−10.79	−30.20	0.88
$\langle U_{LJ} \rangle$	−1.85	−5.27	−11.13	−15.69	0.04
ED−H_2O					
$\langle U_Q \rangle$	−110.36	−95.29	−69.54	−72.20	2.05
$\langle U_{LJ} \rangle$	−8.39	−4.69	0.48	4.39	0.07
H_2O−H_2O					
$\langle U_Q \rangle$	−56.93	−51.74	−38.32	−11.71	0.34
$\langle U_{LJ} \rangle$	8.99	8.69	7.22	2.29	0.03
$\langle U_{tot} \rangle$	**−42.36**	**−32.58**	**−4.21**	**71.79**	**0.01**
AE−AE					
$\langle U_Q \rangle$	−1.68	−4.56	−15.43	−37.54	0.52
$\langle U_{LJ} \rangle$	−1.36	−4.42	−9.84	−13.54	0.03
AE−H_2O					
$\langle U_Q \rangle$	−115.37	−101.28	−76.92	−81.94	2.00
$\langle U_{LJ} \rangle$	−6.07	−2.56	2.61	8.16	0.08
H_2O−H_2O					
$\langle U_Q \rangle$	−56.91	−51.56	−37.87	−10.41	0.33
$\langle U_{LJ} \rangle$	8.98	8.65	7.22	2.19	0.02
$\langle U_{tot} \rangle$	**−44.27**	**−38.80**	**−23.18**	**17.99**	**0.02**

The self-diffusion coefficient (D) is an important dynamical property for the systems of interest. Values of D obtained in the present study are compared with the compositional dependence of experimental estimates in Figure 1. Self-diffusion coefficients for aqueous solutions of EG and ED were measured at 298 K by spin−echo nuclear magnetic resonance (NMR);[46,47] it is unfortunate that there seem to be no experimental results available for binary mixtures of water and AE. Figure 1a shows

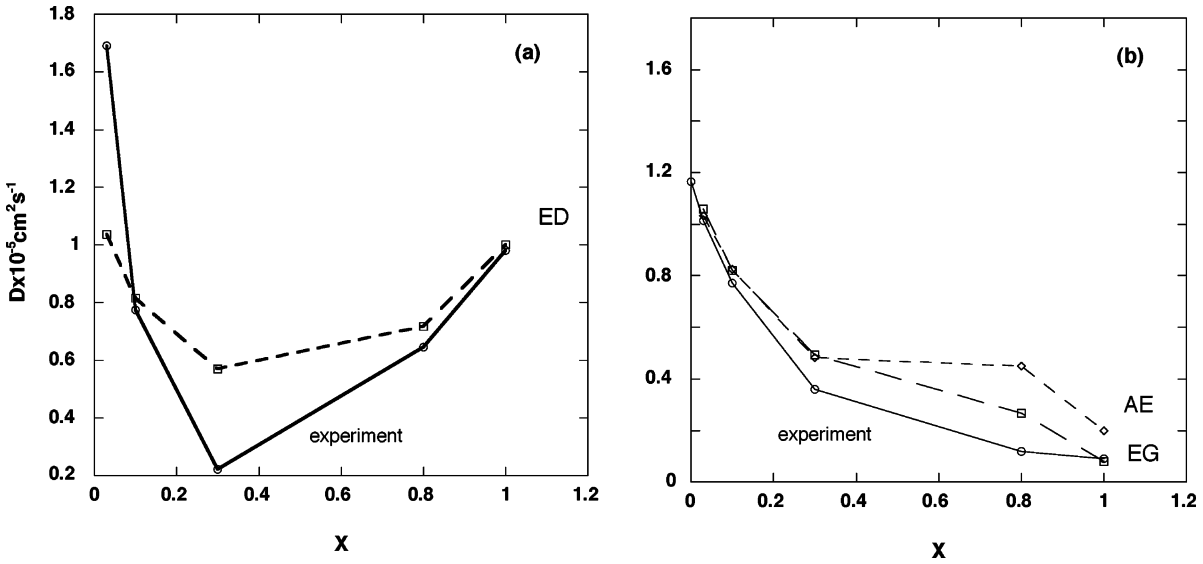

Figure 1. Composition dependence of the solute self-diffusion coefficient (D) in aqueous solutions of ethylene glycol, ethylenediamine, and 2-aminoethanol at 298 K. Panel (a) shows results for ED ((—) experimental and (- - -) present results), whereas panel (b) shows results for (- - -) AE and EG ((—) experimental and (— — —) present results).

that the compositional dependence for ED is, qualitatively, reproduced very well by the present results, in particular the decreasing trend of D up to $X = 0.3$ ($X = 0.33$ in the experimental data). At this concentration, Val'kovskaya et al.[47] observed a minimum in ED mobility and suggested that it corresponds to the formation of cyclic ED·2H_2O complexes.[48] Earlier, the same research group (Rodnikova et al.[49]) studied the dielectric properties of water−ED mixtures and concluded that a molecule of ED is incorporated into the hydrogen-bonded network of water without alteration of the network, up to a concentration of 10 mol %. For aqueous solutions of EG, the experimental D value gradually decreases, becoming essentially constant in EG-rich solutions (i.e., $X > 0.8$ in Figure 1b). The dependence exhibited by the present results is in good quantitative agreement with the experimental curve over essentially the entire range of compositions. Similar trends (also see Figure 1b) have been observed for AE in the water−AE mixtures considered in the present study.

A somewhat unusual increase in D at $X = 0.8$ has been noted for AE (see Figure 1b), as well as for ED solutions. It can be explained by the sensitivity of constant-volume simulations to the quality of the experimental density; even a small (∼5%) error in this parameter can cause significant deviation of the self-diffusion coefficient. To address this problem, the simulations for ED and AE solutions at $X = 0.8$ were conducted under both constant-volume and constant-pressure conditions. The latter conditions do not require experimental densities for the simulation run and, especially in the case of ED solution, the value of D is noticeably improved, as it can be seen from Figure 1a.

In addition, some interesting trends were observed in the compositional dependence of the self-diffusion coefficient for water (not shown). The presence of organic solute significantly decreases the mobility of water molecules, up to $X = 0.3$ for the mixtures of all three compounds. A further increase in solute composition beyond $X = 0.3$ causes a further decrease in D for water in AE and EG mixtures, whereas the corresponding values of D in ED mixtures remain virtually unchanged. For all three solutions, the corresponding values of D approach those of the pure liquids (0.08×10^{-5}, 1.0×10^{-5}, and 0.2×10^{-5} cm^2/s for EG, ED, and AE, respectively[31]). We remark that very good agreement is observed between experimental[46] and the present results for the self-diffusion coefficient of water in EG solutions.

3.2. Dihedral Angle Distributions. Conformational characteristics of aqueous mixtures of EG, ED, and AE were investigated in a manner similar to that used for pure liquids.[31] The dihedral angle distributions were obtained for each concentration of each organic compound (see ref 50), and the corresponding populations of conformers with respect to the central torsion angle were calculated. These results are presented in Table 3. For the sake of computational efficiency, we have not attempted to obtain fully averaged torsional angle distributions, although the lengths of simulations runs were sufficient for sampling all the key conformations.[31]

The most prominent feature of the OCCO dihedral angle distributions of EG (see Table 3) is the presence of a significant population (56%) of T conformers observed at the lowest composition. For this system, the remaining population is comprised of G conformers (35.3%) and a small amount (8.7%) of G′ conformers. For the three other (higher) concentrations, only *gauche* conformers (consistently exhibiting angles of −62.5° and 62.5°) were registered, analogous to the behavior observed for pure EG.

The conformational shift observed in dilute EG solution indicates that, in the presence of a large number of water molecules, the free energies of the G and T conformers become approximately equal, although in water-poor solution, the G conformer is clearly preferred. This issue will be discussed later, in terms of possible preferences for hydrogen-bond formation. Note that these findings are in qualitative accord with the *ab initio* results of Cramer and Truhlar,[19] Nagy et al.,[20] and Hooft et al.,[21] where the presence of both T and G conformers in infinitely dilute solutions of EG was clearly shown. In addition, our *gauche*:*trans* ratio of ∼50:50 seems to be in reasonable quantitative agreement with the 67:33 estimate predicted by Hooft et al.[21]

In the case of ED solutions, the conformational content is quite uniform, with respect to the NCCN torsion angle (see Table 3). Trans conformers predominate at all compositions with a population of ∼70% for low concentration and 85% for high concentration. Note that, similar to EG, the locations of the

TABLE 3: Conformational Characteristics of Ethylene Glycol (EG), Ethylenediamine (ED), and 2-Aminoethanol (AE) in Their Aqueous Mixtures at 298 K

	EG			ED			AE		
	G′	G	T	G′	G	T	G′	G	T
Composition $X = 0.03$									
(%)	8.7	35.3	56.0	5.1	28.3	66.6	50.5	49.5	–
dihedral angle (deg)[a]	−62.5	62.5	177.5	−67.5	67.5	177.5	−57.5	57.5	–
Composition $X = 0.1$									
(%)	71.3	28.7	–	28.3	1.9	69.8	33.8	–	66.2
dihedral angle (deg)[a]	−62.5	62.5	–	−72.5	67.5	177.5	−57.5	–	177.5
Composition $X = 0.3$									
(%)	9.0	91.0	–	7.3	–	92.7	–	100	–
dihedral angle (deg)[a]	−62.5	62.5	–	−67.5	–	182.5	–	57.5	–
Composition $X = 0.8$									
(%)	42.6	57.4	–	–	16.0	84.0	43.4	56.6	–
dihedral angle (deg)[a]	−62.5	62.5	–	–	67.5	177.5	−57.5	57.5	–

[a] All values for dihedral angles correspond to the maximum probability of dihedral angle distributions.

probability maxima for the central dihedral angle remain virtually unchanged when the composition changes.

The dihedral angle distributions for AE−water mixtures (see Table 3) resemble, for the most part, the behavior observed for the pure system, where these similarities are most pronounced for the $X = 0.3$ solution. The conformational pattern for the $X = 0.03$ and 0.8 concentrations exhibit two peaks located in G and G′ positions at 57.5° and −57.5°, respectively. The $X = 0.1$ composition seems to be quite different, with the NCCO distribution exhibiting a significant *trans* population (66.2%) centered at 177.5°, similar to the lowest composition of EG. A second peak on the $X = 0.1$ distribution, comprising 33.8% of the population, is due to G′ conformers. Comparison of the conformational trends typical for AE with those observed for the same functional groups of EG and ED leads us to the conclusion that the specificity of the force field used to describe torsional motion in AE is partially responsible for the noted similarities in dihedral angle distributions.

3.3. Structural Analysis. To our knowledge, a structural analysis of 1,2-disubstituted ethanes within binary aqueous mixtures based on pair correlation functions has not been previously performed. Site−site RDFs are usually used in the examination of liquid structure, although RDFs can provide a complete structural picture only for liquids of spherical particles. Moreover, the fact that averaging over the angular coordinates of the pair distribution functions can often result in the cancellation of contributions from regions of low and high probability at the same distance, but composing different parts of the local structure in solution, further limits the usefulness of RDFs. However, the aqueous binary mixtures of some associating liquids (e.g., methanol, methylamine) have been successfully examined via a structural analysis utilizing both RDFs as well as spatially resolved distribution functions.[3,18] An analogous approach will be performed in the present study, with respect to aqueous mixtures of EG, ED, and AE.

3.3.1. Solution Structure from Radial Distribution Functions (RDFs). Selected RDFs are shown for pure water (Figure 2) and for aqueous solutions of EG, ED, and AE (Figures 3, 5, and 6, respectively) at four different concentrations. Compositional dependence of the total coordination numbers (CNs), calculated with respect to the selected atomic sites for EG solution, is given in Figure 4; complete data tables of the CNs are available in ref 50.

Our analysis begins with EG solution and a comparison of water−water correlations with those of pure water. Figures 2 and 3a show that the first maximum at 2.8 Å in $g(r_{OO})$ increases monotonically as the EG concentration increases. In water-rich mixtures ($X = 0.03$ and 0.1), the main structural features, representing both primary and secondary coordination, are similar to those observed for pure SPC/E water (see Figure 2), indicating that the presence of EG molecules in this concentration range does not seem to influence the hydrogen-bonded network structure of water strongly. In water-poor mixtures ($X = 0.8$), the shift downward of $g(r_{OO})$ at and beyond the first minimum, together with the enhanced first peak, suggests that there is a tendency for the association of a small number of water molecules (e.g., as dimers or small clusters) in this system. A similar phenomenon has been previously observed in water−methanol mixtures.[3]

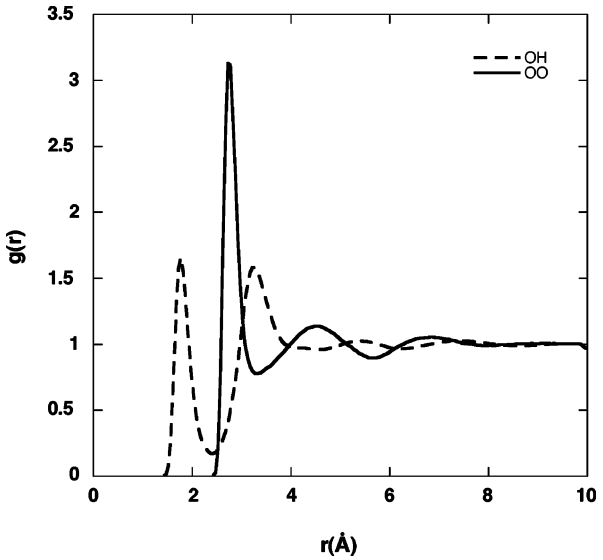

Figure 2. Radial distribution functions for pure SPC/E water at 298 K: (—) the O−O site−site RDFs and (- - -) O−H site−site RDFs.

The first maxima in the EG−EG $g(r_{OO})$, which occurs at 2.8 Å, indicating the presence of strong hydrogen bonding between the corresponding sites, similar to that exhibited in water−water $g(r_{OO})$, increases as the EG concentration decreases, as shown in Figure 3b. This suggests that EG−EG hydrogen bonds persist, even as this component becomes more dilute. The peaks observed in $g(r_{OO})$ at 3.7 Å (with the highest maximum for $X = 0.03$) can be identified with the intramolecular O atom in the *trans* position. We recall that, in dilute solution, the number of molecules in the *trans* conformation increases to ∼50%.

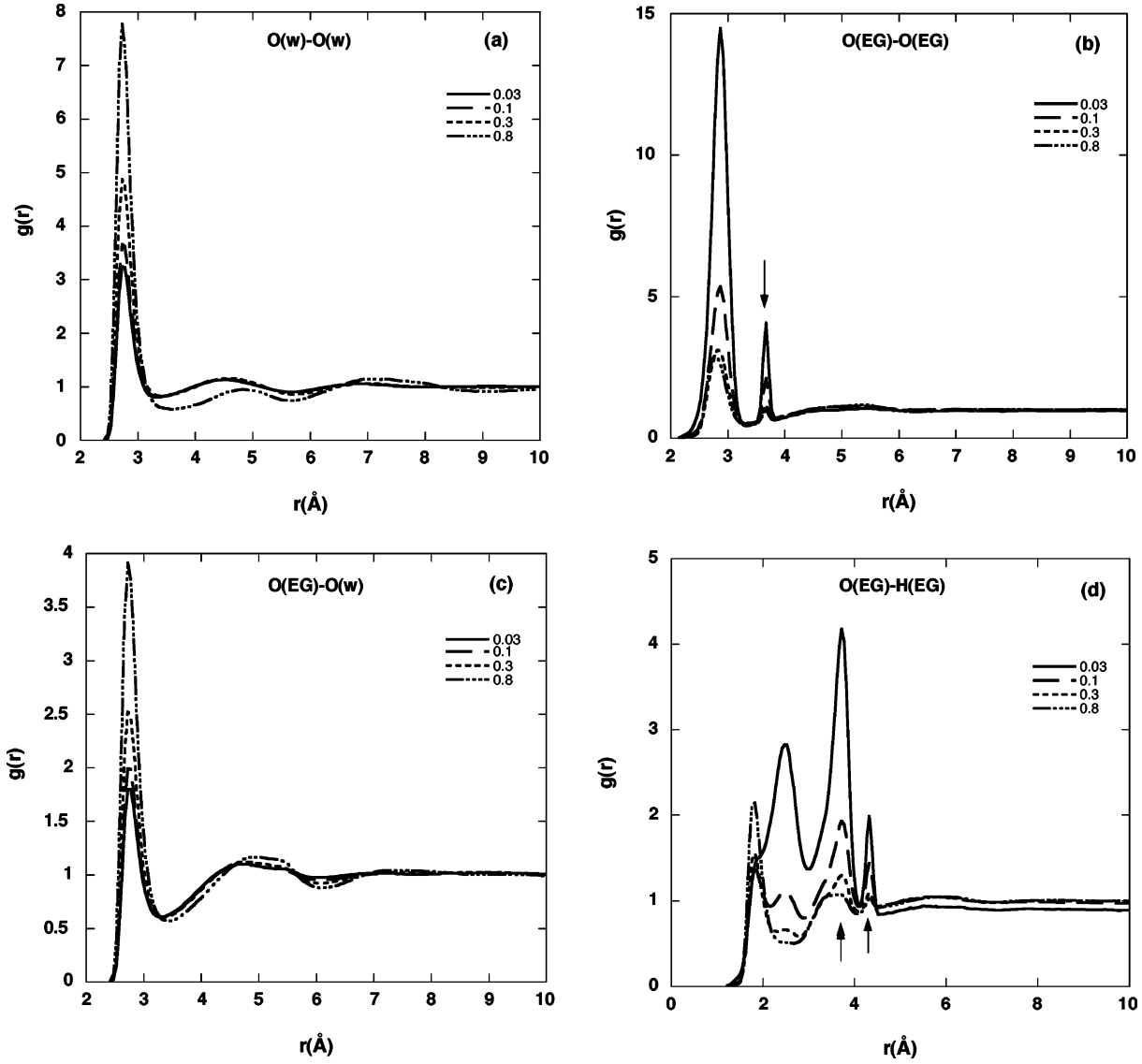

Figure 3. Selected site−site RDFs for water−EG solutions at 298 K: (a) water O−water O, (b) EG O−EG O, (c) EG O−water O, and (d) EG O−EG H. Legend is as follows: (—) $X = 0.03$, (− − −) $X = 0.1$, (- - -) $X = 0.3$, and (− · · · −) $X = 0.08$. Arrows indicate peaks due to intramolecular features.

Results for $g(r_{OO})$ for water−EG pairs are shown in Figure 3c. Overall, the features in these functions become sharper (i.e., higher maxima, deeper minima), indicating strong water−EG correlations as the EG content of these solutions increases. It is also apparent from Figure 3c that the position of the second maximum shifts to slightly larger separations with increasing X, suggesting that there is a change in the specific structure of the second coordination shell in these systems.

The EG O−EG H RDFs for aqueous mixtures of EG (see Figure 3d) are rich in detail and demonstrate the strongest dependence on the concentration. The first peak at 1.8 Å (which is due to relatively strong hydrogen bonding), followed by a less well-defined peak at 3.7 Å (which is due to secondary or intramolecular H atoms from *trans* conformers) can be observed for $X = 0.8$ and 0.3. As the concentration is reduced to <0.3, the peak at 1.8 Å gradually diminishes and, finally, for the most dilute solution, transforms to a small shoulder on a large peak at 2.5 Å, which has been growing after having first appeared at $X = 0.3$. As expected from our conformational analysis, the peak due to intramolecular H atoms of *trans* conformers is a dominant feature in the lowest-concentration solution. The distinct peaks recorded at 4.3 Å, behaving in a similar fashion, can also be identified as an intramolecular feature.

Several features in the estimates of the coordination numbers for water and EG O atoms given in Figure 4 are noteworthy. It might be expected that the coordination numbers around these O atoms would indicate the number of nearest neighbors that are hydrogen-bonded to the central molecule. Figure 4 shows that water maintains a coordination number of CN $\approx$ 4.4 (the same found for pure SPC/E water) until $X = 0.3$, suggesting that the local environment of water molecules is somehow preserved. Beyond this point, the coordination number decreases to CN = 3.9 for the highest concentration of EG. The CNs due to neighboring (hydrogen-bonding) H atoms behave correspondingly; they approach a value of 2 in water-rich solutions (indicating that the two acceptor sites on a water molecule are fully occupied) and then decrease to 1.4 for EG-rich mixtures. This behavior can be interpreted as reflecting the predominant nature of the EG structure in EG-rich aqueous solution when water is unable to establish tetrahedral coordination but rather is forced to adopt a structural motif that is more typical of EG, or at least commensurate with that of EG. The number of

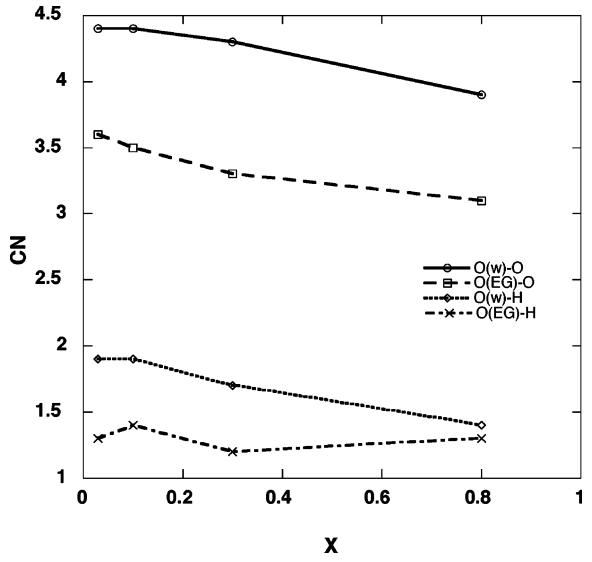

Figure 4. Composition dependence of total coordination number (CN) for aqueous solutions of EG at 298 K: (○) CN around the water O atom due to O atoms, (◇) CN around the water O atom due to H atoms, (□) CN around the EG O atom due to O atoms, and (×) CN around the EG O atom due to H atoms.

neighboring H atoms around an EG O atom remains relatively unchanged over the entire composition range, indicating that the hydrogen-bonding tendency of EG in aqueous solutions does not seem to be particularly sensitive to concentration, in contrast to the behavior found for methanol.[3] Generally, the O atom of water has higher total (see Figure 4) or species-specific (see Table E1 in ref 50) coordination numbers than EG. For example, the total oxygen coordination around water is consistently approximately one greater than that for an EG O atom over the entire composition range.

RDFs for water−ED solutions are shown in Figure 5. The N−O RDFs for ED−water pairs (see Figure 5a) have their first peak at the usual position of 2.8 Å; however, in contrast to the O−O functions for EG−water pairs, the first minimum on the result corresponding to the highest concentration is markedly reduced and shifted toward larger separations. The first maxima (due to apparently strong O−H···N hydrogen bonds) in the corresponding N−H RDFs shown in Figure 5b are very well-defined and are followed by slightly broadened, but also well-defined, secondary maxima at 3.3 Å, after which the functions become essentially featureless. The first minima in this function reach a value of 0.1, indicating a rather stable solute−solvent hydrogen bond when ED acts as the acceptor. In comparison with EG solution, water−water correlations (not shown) did not reveal any unusual structural features; the first peak in $g(r_{OO})$ indicates the presence of strong hydrogen bonding at a separation of 2.7 Å and exhibits a similar trend of increasing intensity in ED-rich mixtures.

The solute−solute correlations are represented by N−N and N−H RDFs (Figures 5c and 5d, respectively). In the former radial function, the first peak is quite distinctive but noticeably shifted toward larger separations, corresponding to a hydrogen-bond length of 2.1 Å. It is followed by a very intense sharp peak that is due to intramolecular nitrogen when an ED molecule adopts a *trans* conformation, with respect to the central dihedral angle. The N−H RDF seems to be the most complicated function for ED−ED pairs (see Figure 5d). Interestingly, similar features and trends apparent in the EG O−EG H RDFs (see Figure 3d) can also be found in $g(r_{NH})$ for ED mixtures. For ED solutions, similar to those of EG, the corresponding RDF curves have four distinct maxima, where they appear at somewhat larger separations for ED. The first peak in $g(r_{NH})$ at 2.1 Å (but only for $X = 0.8$ and 0.3) indicates the presence of somewhat weaker N···H−N hydrogen bonds. At the two lowest concentrations, the disappearance of this first peak is accompanied by the appearance of a broad peak at 2.9 Å, which grows as the ED concentration decreases. Again, analogously to dilute solutions of EG, the largest maximum at 4.1 Å is believed to result from intramolecular H atoms of *trans* conformers. The intensity of this peak correlates well with the population of *trans* conformers present in ED−water mixtures. This population is also "responsible" for the last sharp peak, noted at ∼4.5 Å for both EG and ED solutions.

The coordination numbers provided by the RDFs from ED aqueous solutions reveal further interesting trends (see Table E2 in ref 50). The water oxygen total CNs (due to the presence of both neighboring O atoms from water and nitrogens from ED) for the two water-rich solutions are 4.6, only slightly higher than the 4.4 recorded for pure water and indicating a slight structural "shift" favoring higher coordination (i.e., less tetrahedral). In ED-rich solutions, the CN increases further and approaches a value of 4.8. One possible explanation for this behavior suggests the formation of additional "weak" hydrogen-bond arrangements around the water oxygen acceptor sites to maintain total hydrogen-bond balance in these systems; we recall that, in pure ED,[31] nitrogen has a tendency to participate in two strong and two weak hydrogen bonds to achieve balance, and in ED solution, there will be a shortage of hydrogen-bond acceptor sites. This trend is consistent with the fact that the total hydrogen CNs of the water O atom remain virtually unchanged (∼1.9), indicating that the oxygen acceptor sites continue to be fully occupied. The total coordination around the water O atom is consistently approximately one greater than that for the ED N atom over the entire composition range. This can be explained by noting that both oxygen (in water) and nitrogen (in ED) are double hydrogen-bond donors, whereas nitrogen can accept only a single strong hydrogen bond. As expected, the total hydrogen coordination around ED nitrogen remains relatively constant at ∼1.0.

One might reasonably suggest that the local structural arrangements around OH and NH_2 groups in AE aqueous mixtures would be somewhat reminiscent to those observed around these same groups in EG and ED aqueous solutions. The extent to which this is the case can be considered by examining the RDFs shown in Figure 6 for AE solution. Analysis of water−water correlations (not shown) again reveals a first maximum in $g(r_{OO})$ at 2.8 Å, which increases when the water concentration decreases. As with EG solution, the first minimum in this RDF for AE-rich mixtures is reduced and shifted to slightly larger separations, relative to the functions for the other compositions. As mentioned previously for EG-rich aqueous solutions (see Figure 3a), such structural patterns can be explained by a tendency for the association of small numbers of water molecules, although this behavior is less pronounced in the case of AE. The AE O−water O RDFs (not shown) exhibit a similar tendency of increasing structure with increasing composition, as was observed in the analogous distribution function for EG-rich solution. A trend of increasing peak height with increasing AE composition, somewhat similar to that seen in Figure 3c, can be observed for the RDF for AE N−water O site pairs (see Figure 6a). This function exhibits an initial peak at 2.9 Å, corresponding to strongly hydrogen-bonded nearest neighbors, that increases as the AE composition increases. The growth of secondary features that are also

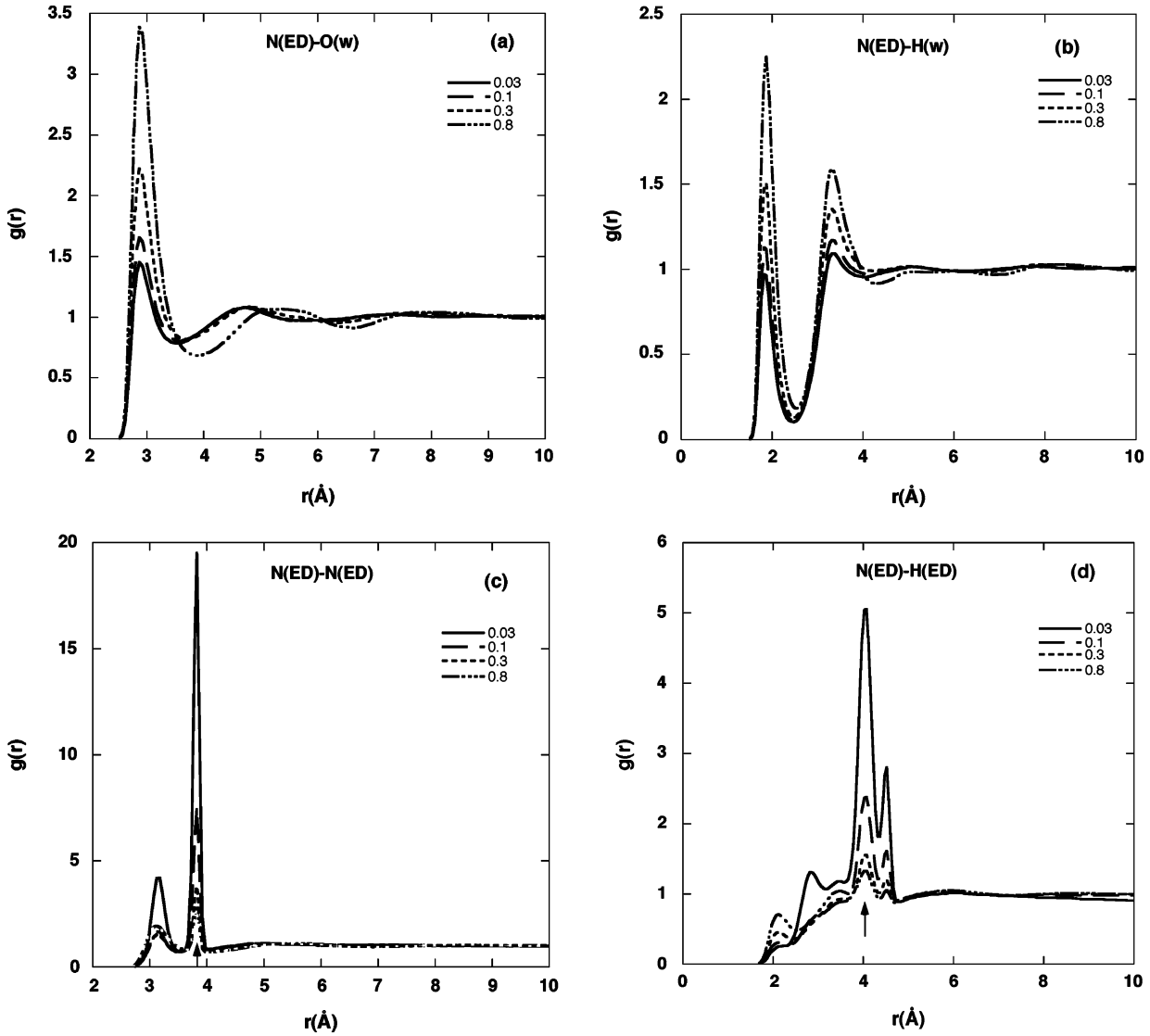

Figure 5. Selected RDFs for water−ED solutions at 298 K: (a) ED N−water O, (b) ED N−water H, (c) ED N−ED N, and (d) ED N−ED H site−site pairs. Legend is as follows: (—) $X = 0.03$, (− − −) $X = 0.1$, (- - -) $X = 0.3$, and (− · · · −) $X = 0.08$. Arrows indicate peaks due to intramolecular features.

noticeably shifted toward large separations can be clearly observed for AE-rich solutions. Such structural patterns are indicative of a rather specific organization of water molecules around the amino group of AE at this composition.

Two further sets of AE−AE RDFs exhibit interesting structural features. The N−amine H RDFs (see Figure 6b) have a small initial peak at 2.1 Å, corresponding to a relatively weak hydrogen bond, which is well-defined only for AE-rich solutions; it rapidly vanishes and transforms to the poorly defined shoulder as the concentration decreases. This RDF also has a second broad peak at 3.5 Å that is at least partially due to the second hydrogen of the hydrogen-bonded NH_2 group. For the three less-concentrated solutions, $g(r_{NH(N)})$ becomes rather featureless, maintaining only a broad peak at 5.9 Å, reflecting the efficacy of water in suppressing apparent solute−solute correlations. From the O−amine H RDF shown in Figure 6c, one can observe that, in contrast to the N−amine-H RDFs of AE but similar to $g(r_{OH})$ of the EG solution, the apparent structure decreases as the AE concentration increases. The first peak at 2.3 Å, which is due to hydrogen bonding in an AE-rich solution, becomes better defined and its maximum shifts to 2.5 Å as the concentration decreases, whereas the position of the second peak (at 3.2 Å) remains virtually unchanged. In water-rich solution, these two features overlap, although they maintain clear maxima; also evident is a barely distinguishable shoulder at 4.4 Å, which is likely due to the internal coordination. The appearance of such a complicated pattern suggests a change in relative importance of intercoordination versus intracoordination with compositional change, where it is presumably the latter that dominates in water-rich solution.

For the sake of comparison with the analogous RDFs of EG solution, the AE−AE $g(r_{OO})$ is shown in Figure 6d. The trend observed in the height of the first peak is opposite to that noted for EG mixtures, i.e., a decrease of intensity with decreasing concentration. This observation indicates that increased hydration is disruptive to O−O (unlike O−N) relative coordination for AE molecules.

Comparison of the detailed numerical results for the CNs for AE mixtures with the appropriate CNs for aqueous EG and ED solutions reveals more apparent similarities than differences. For instance, similar to EG, the total number of O and N atoms around the water O atom remains virtually unchanged at essentially 4.4 over the entire composition range (we recall that it increased only slightly for ED mixtures). The total number of H atoms around the water O atom also remains almost unchanged, starting at 1.9 for water-rich compositions and

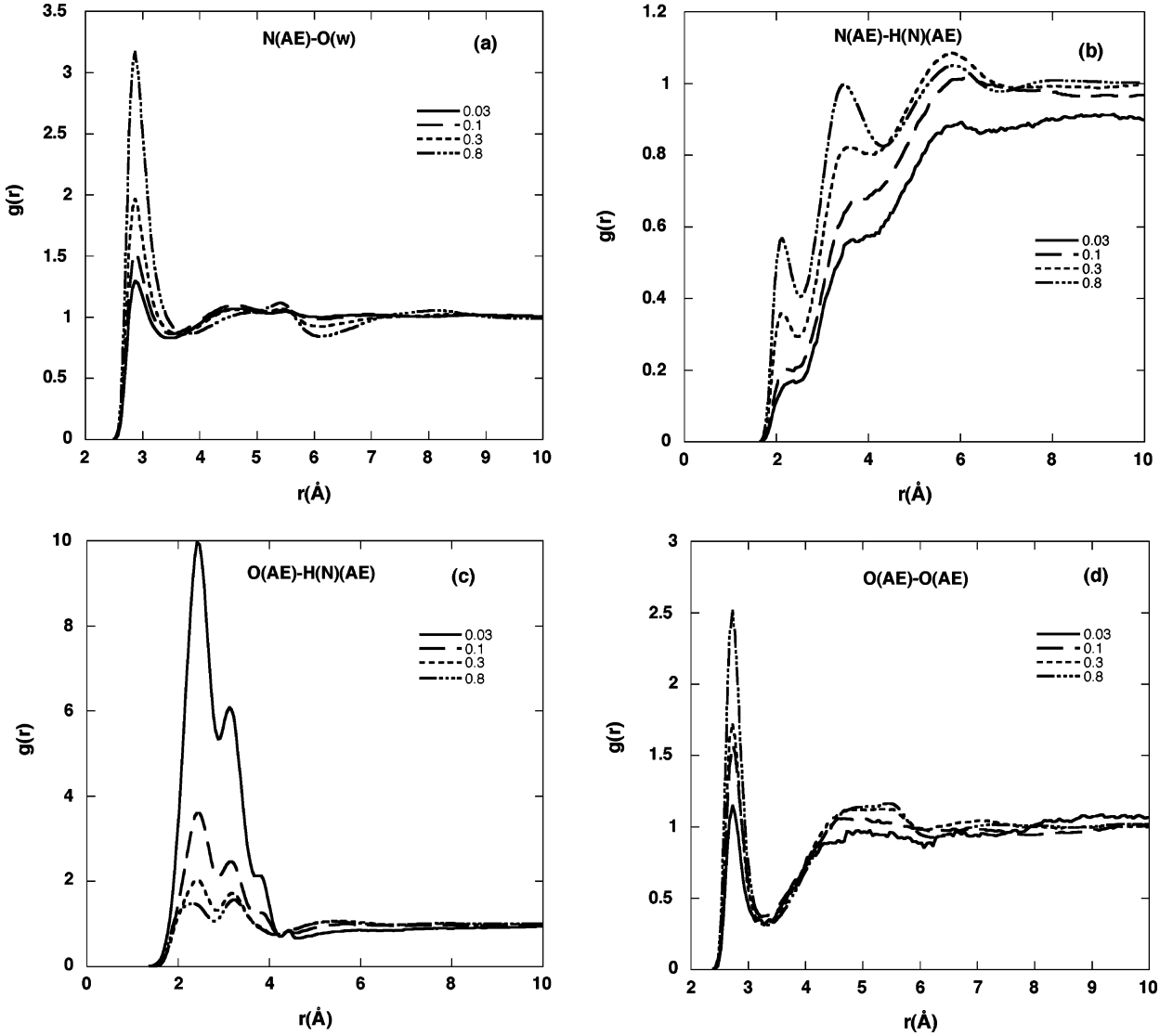

Figure 6. Selected RDFs for water−AE solution at 298 K: (a) AE N−water O, (b) AE N−AE H, (c) AE O−AE H, and (d) AE O−AE O site−site pairs. Legend is as follows: (—) $X = 0.03$, (− − −) $X = 0.1$, (- - -) $X = 0.3$, and (− • • • −) $X = 0.08$.

decreasing only slightly to 1.7 for an AE-rich solution. This trend seems to be far less extreme than that reported for aqueous solutions of methanol[3] or *tert*-butyl alcohol.[51]

Similar to the water O atom, the total coordination around the AE O atom remains virtually unchanged over the entire composition range (see Table E3 in ref 50). The estimates for various site-specific CNs in AE-rich mixtures correlates well with the appropriate CN for pure AE.[31] For all four solutions studied, the sum of the total coordination around both AE N and O atoms is 7.5; this value is ∼0.5 higher than that obtained for pure AE. Together, these observations imply that the local hydrogen-bonding structure around an AE molecule in its aqueous mixtures is somewhat affected by the composition of the mixture. A structural analysis using SDFs has been performed to add more details to the qualitative picture previously described.

3.3.2. Solution Structure Revealed by Spatial Distribution Functions (SDFs). In the present SDF analysis, the site-specific local structure and its dependence on concentration were examined for aqueous solutions of EG, ED, and AE. The sets of SDFs, which are representative of the local water structure around (1) a water molecule and (2) an organic molecule in the solutions of interest, as well as the local structure of organic compound around (3) water and (4) the corresponding ethane derivative, were visualized and systematically studied. A representative sampling of the most typical, the most unusual, or the most interesting examples selected from these sets are presented in Figures 7−14.

The compositional behavior of the local water structure around a water molecule, as measured by the O−O SDFs for EG, ED, and AE solutions, reveals more similarities than differences. Two water−water SDFs for $X = 0.03$ and 0.3 solutions of AE are shown in Figure 7. At an isosurface threshold of 1.6 times that of the bulk, one can see three principal features that are very reminiscent of those observed in pure water:[1] the two distinct caps centered directly over the H atoms of the central molecule, which are due to its hydrogen-bond-accepting neighbors, and the single large feature below the central molecule, which is due to its two hydrogen-bond-donating neighbors. The two more-distant features in Figure 7a indicate the presence of additional ("interstitial") coordination that is also found in the pure liquid.[1] Results at the same threshold for dilute EG and ED solutions (not shown) seem to be almost identical to those in Figure 7a. At higher concentrations (see Figure 7b), one can begin to see the appearance of a secondary structure consisting of two large hemispherical caps

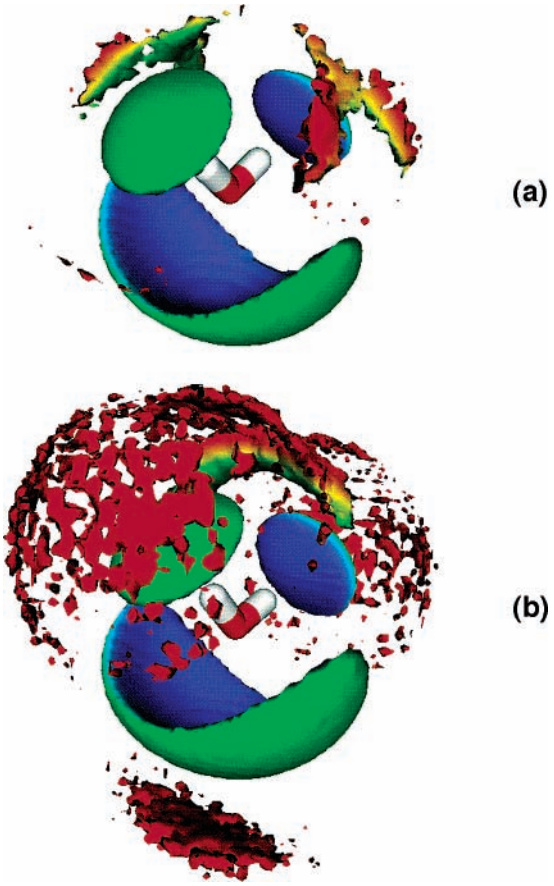

Figure 7. Local water structure around a water molecule in AE solution at 298 K, as measured by the O−O SDF, for a mole fraction of (a) $X = 0.03$ and (b) $X = 0.3$. The isosurface threshold is 1.6 times that of the bulk. The surfaces are colored based on separation, from 2.5 Å (dark blue) to 4.0 Å and larger (red).

surrounding the principal hydrogen-bond-accepting features (which overlap to form a ridge located along the bisecting plane above the two caps) and a single feature below the principal hydrogen-bond-donating neighbors. We note that the unusual ridgelike feature is only clearly apparent for the $X = 0.3$ solution of AE.

Spatial density maps of EG O atoms and ED N atoms around the water O atom, in corresponding EG and ED solutions at low and high compositions, are shown in Figures 8 and 9, respectively, at a threshold of 1.6. Figure 8a shows that the principal donating feature around a water molecule is split into two shallow caps, indicating that, in the case of dilute EG solution, a water molecule prefers to accept a hydrogen bond from EG at a tetrahedral rather than dipolar (axial) position. This preference for tetrahedral coordination becomes especially pronounced in dilute ED solution (see Figure 9a), where it manifests itself in two rather distorted (somewhat triangular) caps below each of the "lone pair" sites. This behavior can be explained by again considering the balance of hydrogen-bond donor and acceptor sites. With an excess of donor sites in ED solutions, it would seem that water, when it hydrogen-bonds to the N atom, strongly prefers to utilize fully both of its acceptor sites. One further similarity can be noted between Figures 8a and 9a. These are the two equatorial out-of-plane features that represent the tendency of a water molecule hydrating the CH_2 groups (adjacent to the respective O or N atoms of EG or ED molecules, respectively) to lie flat on these hydrophobic surfaces. At the threshold used in Figures 8a and 9a (1.6), these features are just beginning to appear for these dilute solutions.

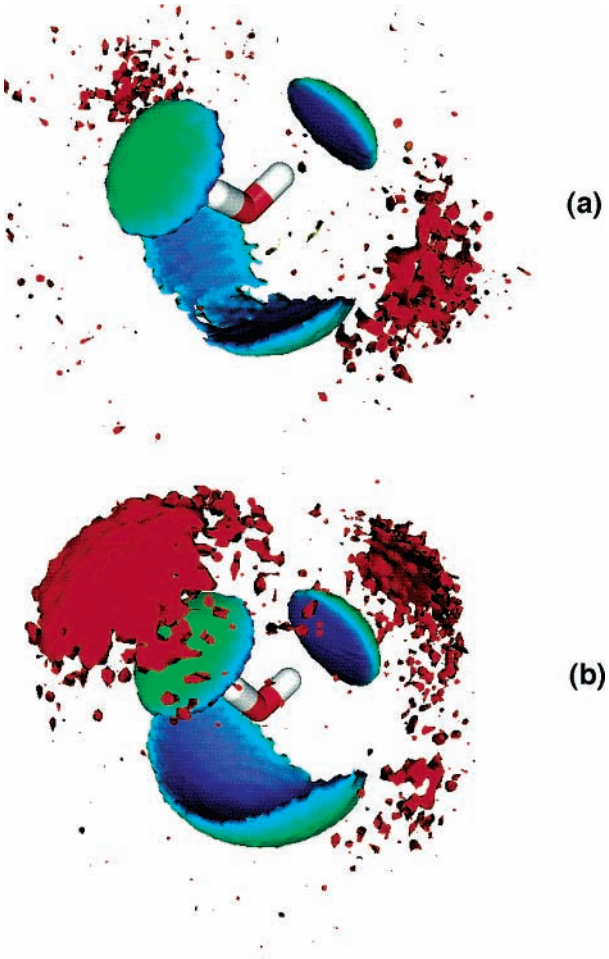

Figure 8. Spatial density of EG O atoms around the water O atom in EG solutions at 298 K, for a mole fraction of (a) $X = 0.03$ and (b) $X = 0.8$. The isosurface threshold is 1.6 times that of the bulk. The surfaces are colored based on separation, as in Figure 7.

At high concentration (see Figures 8b and 9b), the hydration picture changes dramatically. The tendency for tetrahedral coordination seems to be lost for both EG and ED, as well as the out-of-plane hydrophobic hydration features. Moreover, for EG solution, the appearance of secondary caps above the principal hydrogen-bond-donating features in Figure 9b is further indication of a clear trend to hydrophilic hydration at high concentration, i.e., for water molecules to prefer to associate with the hydrogen-bonding groups ("heads") of these molecules. As mentioned previously, the specific behavior of water molecules noted in Figures 8a and 9a for dilute solutions serves as evidence of hydrophobic hydration of the remainder of the organic molecule. This trend seems to be in good qualitative agreement with results reported by Hata and Ono,[52] who analyzed, by means of SDF, the hydration structure of five of the most abundant conformers in liquid EG; they also observed features that were due to hydrophobic hydration (so-called HH regions[52]) in infinitely dilute solution of this compound.

We note that the water−solute structure in AE solution (not shown) is very reminiscent of that observed for the corresponding functional groups in EG and ED solutions. However, there are some subtle differences. For instance, the water O−AE O SDF measured at the highest concentration ($X = 0.8$) still exhibits the presence of some hydrophobic structural arrangements, which is not evident in Figure 5b for the EG solution.

The local water structure around organic molecules (in particular, around the hydroxyl groups of EG and AE and the

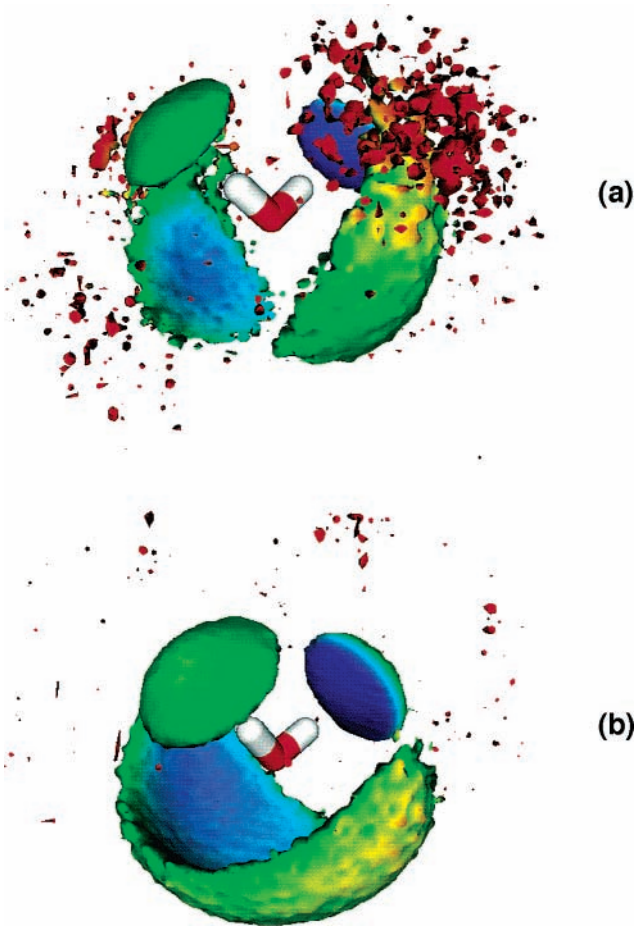

Figure 9. Spatial density of ED N atoms around the water O atom in ED solutions at 298 K, for a mole fraction of (a) $X = 0.03$ and (b) $X = 0.8$. The isosurface threshold is 1.6 times that of the bulk. The surfaces are colored based on separation, as in Figure 7.

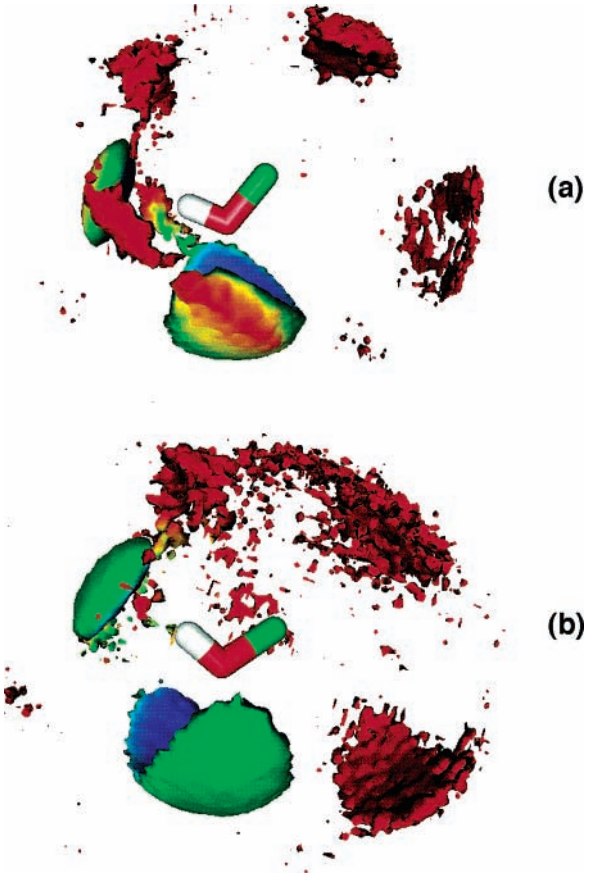

Figure 10. Local water structure around hydroxyl groups in dilute solutions ($X = 0.1$) of (a) EG and (b) AE at 298 K, as measured by the O−O SDFs. The isosurface thresholds are 1.8 and 1.9 times that of the bulk, respectively. The surfaces are colored based on separation, as in Figure 7.

amino groups of ED and AE) is displayed in Figures 10 and 11. In Figure 10a, the EG O−water O SDF for an EG solution at $X = 0.1$ (still considered to be low concentration) exhibits a primary hydrogen-bonding pattern that is very similar to that observed for pure EG (see Figure 5b of ref 31, where the same isosurface threshold allows for direct comparison). The rim on the lower edge of the principal donating feature, as well as two apparent "wings" that appear as small separate features in equatorial positions, with respect to the central hydroxyl, are the most-prominent additional features in Figure 10a. They suggest the presence of weakly hydrogen-bonded nearest water O atoms and serve as evidence that, even in dilute aqueous solution, the EG O atom exhibits a hydrogen-bonding pattern that is similar to that found in the pure system. In contrast to EG, for the AE hydroxyl (see Figure 10b), only principal hydrogen-bonded features are apparent; it is not possible to localize weakly bonded nearest neighbors, as was also the case for pure liquid AE.

The local water structure around the amino group is shown in Figures 11a and 11b for $X = 0.3$ solutions of ED and AE, respectively, where the corresponding N−water O SDFs are visualized at thresholds of 1.8 and 2.0, respectively. In Figure 11a, the primary hydrogen-bonded features are clearly evident as caps over each of the two H atoms and as a slightly elongated feature immediately below the amino group. The ridge extending between the two amino H caps is particularly interesting, because it represents a bridging second-neighbor water molecule. It can be expected that this water forms (likely strong) hydrogen bonds with the two neighbors occupying the primary hydrogen-bond-acceptor positions over the amino group. An analogous hydrogen-bonding arrangement around an amino group was observed previously in aqueous solutions of methylamine.[18] Also note that this SDF allows one to see clearly all the primary hydrogen-bonded features (both donors and acceptors), because of the hydration of the second intramolecular N atom when an ED molecule adopts a *trans* conformation. The principal hydration pattern around the amino group in AE solution (see Figure 11b) is quite similar to that shown in Figure 11a, with exception of the secondary features associated with the intramolecular O atom in *gauche* position. Moreover, the presence of a "bridge" located above the central N atom and appearing as an extension of the accepting caps leading toward the secondary (intramolecular) features is also noteworthy. It could be indicative of a first (weak) hydrogen-bonding water neighbor, which is necessary to maintain proper hydrogen-bond balance and forced to occupy a rather unexpected position because of the internal geometry of the AE molecule; this water molecule is attempting to bridge the hydroxyl and amino groups of a molecule in the *gauche* conformation.

Spatial solute−solute correlations for dilute and concentrated solutions of EG, ED, and AE are shown in Figures 12, 13, and 14, respectively. All features evident in Figure 12, which are due to both first- and second-nearest neighbor atoms, can be immediately recognized when compared with those identified for pure EG.[31] Thus, the presence of water seems to have had little qualitative effect on the structural preferences of EG around another EG molecule. At the highest concentration ($X = 0.8$),

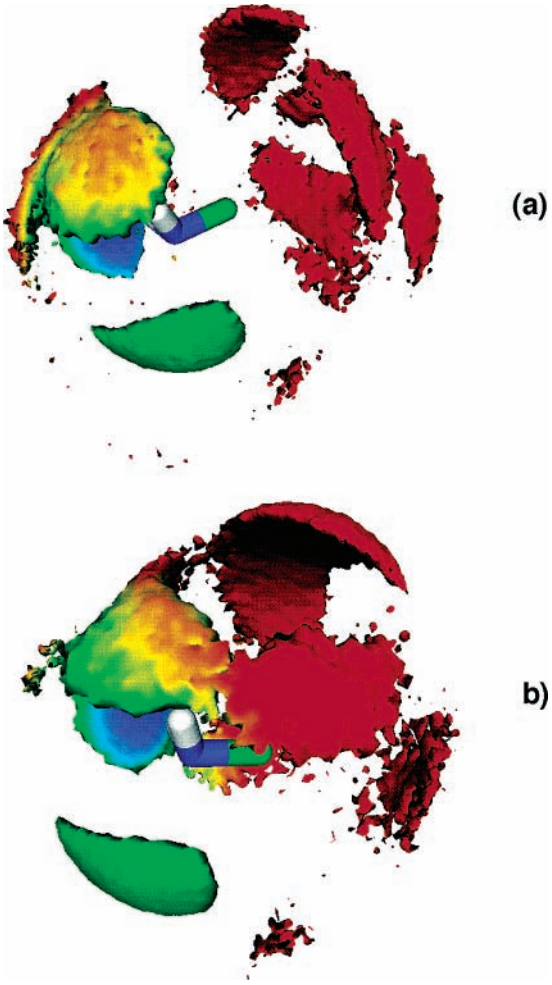

Figure 11. Local water structure around the amino groups in $X = 0.3$ solutions of (a) ED and (b) AE at 298 K, as measured by the N−O SDFs. The isosurface thresholds are 1.8 and 2.0 times that of the bulk, respectively. The surfaces are colored based on separation, as in Figure 7.

the N−N SDF for ED (see Figure 13b) and all four N and O SDFs for AE (only O−N is shown in Figure 14a) essentially reproduce the main structural patterns found in the respective pure liquids.[31] The only exception to this is the coordination of the second amino group of the *trans* conformers in ED solution. However, further analysis of the main SDF maxima for all compositions, based on variation of the isosurface thresholds, reveals a consistent weakening of solute−solute correlations with increasing water content (even in the presence of only a small number of water molecules). Clearly, water seems to be effectively mediating the direct hydrogen-bond interactions between these organic molecules.

A somewhat surprising change can be noted in the AE O−AE N SDF when the AE concentration decreases to $X = 0.3$ (or lower). Comparing Figures 14a and 14b, one can see that the principal hydrogen-bond-donating feature below its hydroxyl group has a tendency to split into two large caps upon dilution, indicating that the hydroxyl group is better able to utilize both its hydrogen-bond acceptor sites. This observation suggests that the aqueous media is a more accommodating (hydrogen-bonding) environment for the AE molecule than is its pure liquid (allowing for better utilization of the hydrogen-bonding sites).

Finally, previous experimental findings[46] have suggested that the amphiphilic character of these representatives of 1,2-disubstituted ethanes can lead to a certain degree of association

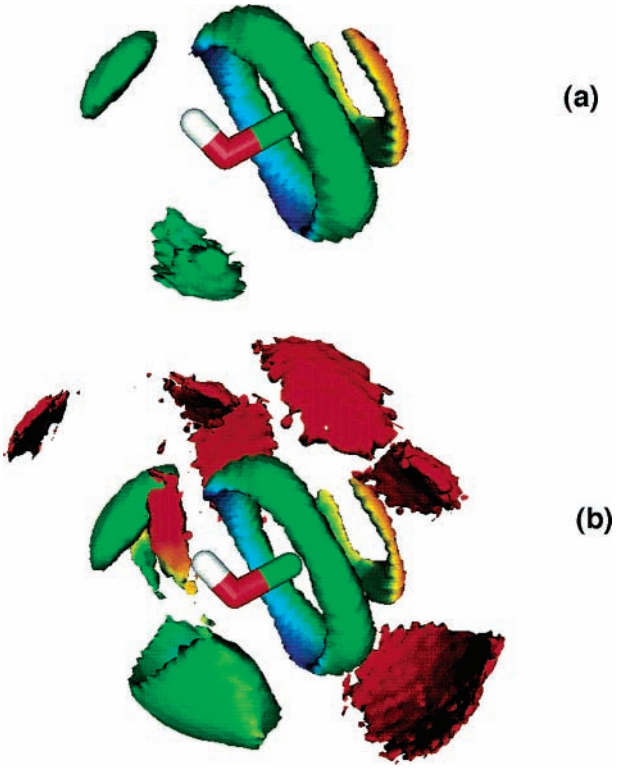

Figure 12. EG O−EG O spatial distribution functions in (a) dilute ($X = 0.1$) and (b) concentrated ($X = 0.8$) EG solutions at 298 K. The isosurface thresholds are 3.0 and 1.6, respectively. The surfaces are colored based on separation, as in Figure 7.

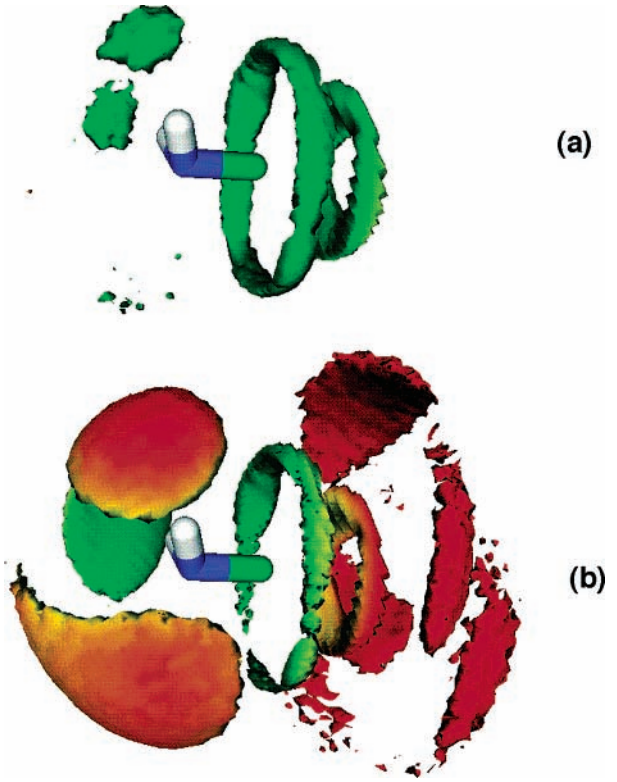

Figure 13. ED N−ED N SDFs in (a) dilute ($X = 0.1$) and (b) concentrated ($X = 0.8$) ED solutions at 298 K. The isosurface thresholds are 3.0 and 1.6, respectively. The surfaces are colored based on separation, as in Figure 7.

in aqueous solutions. To investigate this suggestion, we have examined solute C−solute C and solute C−water O SDFs (not

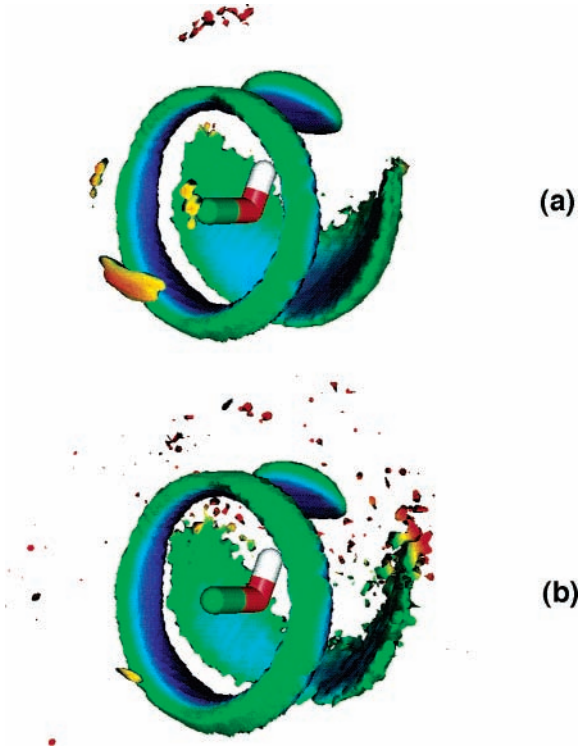

Figure 14. AE O−AE N SDFs in AE aqueous solutions at 298 K: (a) mole fraction of $X = 0.8$ and (b) mole fraction of $X = 0.3$. The isosurface threshold of 2.0 is shown. The surfaces are colored based on separation, as in Figure 7.

shown) for each composition of aqueous EG, ED, and AE. The C−C SDFs measured at a threshold of 2.0 for ED exhibits a broad ring around the hydrophobic portion of the ED molecule (which adopts primarily the *trans* conformation in all aqueous solutions). A similar picture is observed for AE at $X = 0.1$, which is the only composition that also exhibits a significant amount of *trans* rotamers. Such a local density pattern indicates the presence of multiple nonspecific hydrophobic contacts, that is, the *tendency* of association between hydrophobic chains of ED and AE molecules in "open" (i.e., *trans*) conformation. The previously described association seems to be quite different from that observed by Kusalik et al.[51] in *tert*-butyl alcohol (TBA) aqueous solutions, where the preferred areas of association were definitely localized and the high thresholds (of 4.5−6.0 times the average density) reflect the strong association of TBA molecules.[51] One might expect somewhat similar behavioral patterns to be observed, for instance, in the case of higher members of the diol or diamine series, in which the absence of intramolecular hydrogen bonding as well as the increased length of the aliphatic chain would alter the interplay between hydrogen bonding and hydrophobic interactions. The major difference observed in the C−water O SDFs of all three compounds occurs when low and high concentrations are compared and results from the presence of water molecules coordinated to the hydrophobic portion of the organic molecules in water-rich solutions. It is believed that this water may also help (beyond hydrogen-bond consideration) to stabilize specific conformations of EG, ED, and AE molecules at low concentrations.

4. Conclusions

In this paper, the investigation of ethylene glycol (EG), ethylenediamine (ED), and 2-aminoethanol (AE)[31] is extended to their aqueous mixtures. On the basis of simulations and the analysis previously performed for pure liquids, three united-atom OPLS-based potential models with fixed bond lengths were chosen for simulations of aqueous solutions. The rigid SPC/E water potential was used as the molecular model for water. For each system, four compositions (organic solute mole fractions of 0.03, 0.1, 0.3, and 0.8) spanning the full range of concentrations were prepared. Molecular dynamics (MD) computer simulations were then performed for these model binary aqueous mixtures. Subsequent trajectory analysis included the accumulation of radial distribution functions (RDFs) and spatial distribution functions (SDFs), as well as average configurational energies and self-diffusion coefficients.

Dihedral angle distributions, with respect to the torsion angles, were determined for each system and the relative populations of conformers (for the central dihedral angle only) were examined. In the case of AE and EG solutions, these molecules essentially maintain *gauche* conformation, as was observed for their pure liquids, when in moderate to high concentration. However, for low concentrations, each of these molecules exhibited some tendency to appear in *trans* form. For moderate to high concentrations, ED also behaves similarly to its pure liquid in preferring the *trans* conformation. In dilute aqueous solution, there is an apparent elevation (to ∼30%) in the proportion of *gauche* rotamers. Clearly, the hydrating water influences the existence of the internal hydrogen bond that stabilizes *gauche* conformers. For ED at low concentrations, hydration seems to favor the "closed" (i.e., *gauche*) molecular form, whereas for AE and EG, hydration seems to enhance the likelihood of the "open" (i.e., *trans*) structures. The absence of experimental conformational data for these aqueous solutions made the corresponding comparison impossible; however, for a dilute solution of EG, excellent agreement was achieved with a previously reported theoretical result.[21]

The quality of the molecular models used in the present simulations of aqueous solutions was also confirmed by results obtained for the self-diffusion coefficient (D). To our knowledge, these are the first theoretical estimates of this dynamical property for the aqueous solutions studied. The compositional dependence of the self-diffusion coefficients for the EG and ED, as well as that of water, agreed well with experimentally determined curves. Unfortunately, no experimental data were available for AE. The self-diffusion coefficients for EG and AE were observed to decrease with increasing composition, whereas the results for ED exhibited a minimum at $X = 0.3$, in accord with experiment.[47] An obvious structural origin for the behavior of ED was not identified; however, there was some evidence for the association of the "open" carbon chains of ED at this intermediate composition. As expected, the mobility of the water molecules, as measured by its self-diffusion coefficient, gradually decreases as the concentration of the organic solutes increases.

On the basis of RDF and SDF analysis of the aqueous solutions of EG, ED, and AE, a three-dimensional picture of the local structure around these solute molecules, somewhat analogous to that found in their pure liquids, was revealed. This picture exhibits three- and four-membered arrangements around a central hydrogen-bonding group with the latter becoming dominant at low composition. Both strongly and weakly hydrogen-bonded nearest neighbors were identified. Further interesting trends were noted that were associated with the behavior of water acting as a solvation medium. There is a clear tendency for the association of a small number of water molecules in water-poor aqueous mixtures with EG or AE, as a result of the strong hydrophilic hydration of the hydroxyl and amino groups of these molecules. The preference of water

molecules to lie flat next to the hydrophobic surface of CH_2 groups was apparent, particularly at low concentrations. Water seems to maintain its tetrahedral coordination for all three mixtures over most of the concentration range. The analysis of water-solute structural arrangements revealed a dominance of hydrophilic hydration at high concentrations, whereas in dilute solutions, hydrophobic hydration also becomes clearly evident for all three organic solutes. Solute−solute structure is primarily characterized by weakening of the intensity of all the principal SDFs maxima as composition is decreased, indicating a clear preference for each of the organic molecules to be hydrated rather than self-associated. This behavior is unlike that previously observed in aqueous solutions of methanol[3] or *tert*-butyl alcohol.[51]

Comparison of the present results with those reported in the literature for aqueous solutions of relatively simple nonelectrolytes[3,18,51] revealed some similarities (e.g., the local structure around the amino groups of methylamine, ED, and AE) and differences (e.g., the lack of specific structural features corresponding to "structure making" in water and the absence of self-association of solutes). The latter are consistent with the general observation that these particular disubstituted ethanes seem to be relatively well-accommodated within a water structural network. As in previous work, it was found that hydrogen-bond balance plays a key role in determining the preferred local structures around hydrogen-bonding molecules. It was also shown that the information obtained from RDFs is not sufficient to elucidate fully the local structure in the solutions studied. The ability of SDFs to provide essential detailed insights into the local structural environment of strongly associated molecular liquids has again been demonstrated. However, the conformational flexibility (i.e., the presence of three dihedral angles) of EG, ED, and AE does not always allow localization and identification of all the neighboring atoms. This problem can be partially resolved by producing SDFs for certain (fixed) conformers; such an approach has been previously explored[52] but it requires prior knowledge of the set of important conformations. A more general approach would be to generate atomic density maps with the inclusion of three-body correlations, that is, allow critical conformational information (such as the presence of an intramolecular hydrogen bond) to be available within the recorded data.

Acknowledgment. A.G. thanks Dr. A. Laaksonen and Dr. A. Lyubartsev for providing assistance in the utilization of M.DynaMix simulation package. This work has been supported by the Natural Science and Engineering Research Council of Canada (NSERC).

References and Notes

(1) Kusalik, P. G.; Svishchev, I. M. *Science* **1994**, *265*, 1219.
(2) Svishchev, I. M.; Kusalik, P. G. *J. Chem. Phys*. **1994**, *100*, 5165.
(3) Laaksonen, A.; Kusalik, P. G.; Svishchev, I. M. *J. Phys. Chem.* **1997**, *101*, 5910.
(4) Bergman, D. L.; Laaksonen, A. *Mol. Simul*. **1998**, *20*, 245.
(5) Bergman, D. L.; Laaksonen, L.; Laaksonen, A. *J. Mol. Graphics Modell*. **1997**, *15*, 301.
(6) Bergman, D. L.; Laaksonen, A. *Phys. Rev. E* **1998**, *58*, 4706.
(7) Vishnyakov, A.; Widmalm, G.; Kowalewski, J.; Laaksonen, A. *J. Am. Chem. Soc*. **1999**, *121*, 5403.
(8) Jorgensen, W. L.; Madura, J. D. *J. Am. Chem. Soc*. **1983**, *105*, 1407.
(9) Soper, A. K.; Finney, J. L. *Phys. Rev. Lett.* **1993**, *71*, 4346.
(10) Dunn, W. J.; Nagy, P. I. *J. Phys. Chem*. **1990**, *94*, 2099.
(11) Dunn, W. J.; Nagy, P. I.; Collantes, E. *J. Am. Chem. Soc*. **1991**, *113*, 7898.
(12) Nagy, P. I. *Acta Chim. Hung.* **1992**, *129*, 429.
(13) Kawata, M.; Ten-no, S.; Kato, S.; Hirata, F. *Chem. Phys*. **1996**, *203*, 53.
(14) Morgantini, P. Y.; Kollman, P. A. *J. Am. Chem. Soc*. **1995**, *117*, 6057.
(15) Spector, T. I.; Kollman, P. A. *J. Phys. Chem. B* **1998**, *102*, 4004.
(16) Rizzo, C. R.; Jorgensen, W. L. *J. Am. Chem. Soc*. **1999**, *121*, 4827.
(17) Impey, R.; Sprik, M.; Klein, M. *J. Am. Chem. Soc*. **1987**, *109*, 5900.
(18) Kusalik, P. G.; Bergman, D.; Laaksonen, A. *J. Chem. Phys*. **2000**, *113*, 1.
(19) Cramer, C. J.; Truhlar, D. G. *J. Am. Chem. Soc*. **1994**, *116*, 3892.
(20) Nagy, P. I.; Dunn, W. J., III; Alagona, G.; Ghio, C. *J. Am. Chem. Soc*. **1991**, *113*, 6719.
(21) Hooft, R. W. W.; van Eijck, B. P.; Kroon, J. *J. Chem. Phys*. **1992**, *97*, 3639.
(22) Alagona, G.; Ghio, C. *J. Mol. Struct. (THEOCHEM)* **1992**, *254*, 287.
(23) Varnek, A. A.; Wipff, G.; Glebov, A. S.; Feil, D. *J. Comput. Chem*. **1995**, *16*, 1.
(24) Jorgensen, W. L. *J. Phys. Chem*. **1986**, *90*, 1276.
(25) Jorgensen, W. L.; Madura, J. D. *Mol. Phys*. **1985**, *56*, 1381.
(26) van Gunsteren, W. F.; Berendsen, H. J. C. *Groningen Molecular Simulation (GROMOS)*; Library Manual: Groningen, The Netherlands, 1987.
(27) Berendsen, H. J. C.; Posta, J. P. M.; van Gunsteren, W. F.; Hermans, J. *Intermolecular Forces*; Reidel: Dordrecht, The Netherlands, 1985.
(28) Miertus, S.; Scrocco, E.; Tomasi, J. *Chem. Phys*. **1981**, *55*, 117.
(29) Pachler, K. G. R.; Wessels, P. L. *J. Mol. Struct*. **1970**, *6*, 471.
(30) Krueger, P. J.; Mettee, H. D. *J. Mol. Spectrosc.* **1965**, *18*, 131.
(31) Gubskaya, A. V.; Kusalik, P. G. *J. Phys. Chem. A* **2004**, *108*, 7151.
(32) Cornell, W. D.; Cieplak, P.; Bayly, Ch. I.; Kollman, P. A. *J. Am. Chem. Soc*. **1993**, *115*, 9620.
(33) DeBolt, S. E.; Kollman, P. A. *J. Am. Chem. Soc*. **1995**, *117*, 5316.
(34) Tirado-Rives, J.; Jorgensen, W. L. *J. Am. Chem. Soc*. **1990**, *112*, 2773.
(35) Berendsen, H. J. C.; Grigera, J. R.; Straatsma, T. P. *J. Phys. Chem*. **1987**, *91*, 6269.
(36) Lyubartsev, A. P.; Laaksonen, A. *Comput. Phys. Commun*. **2000**, *128*, 565.
(37) Allen, M. P.; Tildesley, D. J. *Computer Simulation of Liquids*; Clarendon Press: Oxford, U.K., 1987.
(38) Ryckaert, J.-P.; Ciccotti, G.; Berendsen, H. J. C. *J. Comput. Phys*. **1977**, *23*, 327.
(39) Ivanova, E. F.; Kiiko, S. M. *Visn. Khark. Univ.* **1993**, *378*, 92. (Journal written in Russian.)
(40) Aminabhavi, T. M.; Gopalakrishna, B. *J. Chem. Eng. Data* **1995**, *40*, 856.
(41) Maham, Y.; Teng, T. T.; Hepler, L. G.; Mather, A. E. *J. Solution Chem*. **1994**, *23*, 195.
(42) Frisch, M. J.; Trucks, G. W.; Schlegel, H. B.; Scuseria, G. E.; Robb, M. A.; Cheeseman, J. R.; Zakrzewski, V. G.; Montgomery, J. A., Jr.; Stratmann, R. E.; Burant, J. C.; Dapprich, S.; Millam, J. M.; Daniels, A. D.; Kudin, K. N.; Strain, M. C.; Farkas, O.; Tomasi, J.; Barone, V.; Cossi, M.; Cammi, R.; Mennucci, B.; Pomelli, C.; Adamo, C.; Clifford, S.; Ochterski, J.; Petersson, G. A.; Ayala, P. Y.; Cui, Q.; Morokuma, K.; Malick, D. K.; Rabuck, A. D.; Raghavachari, K.; Foresman, J. B.; Cioslowski, J.; Ortiz, J. V.; Stefanov, B. B.; Liu, G.; Liashenko, A.; Piskorz, P.; Komaromi, I.; Gomperts, R.; Martin, R. L.; Fox, D. J.; Keith, T.; Al-Laham, M. A.; Peng, C. Y.; Nanayakkara, A.; Gonzalez, C.; Challacombe, M.; Gill, P. M. W.; Johnson, B. G.; Chen, W.; Wong, M. W.; Andres, J. L.; Head-Gordon, M.; Replogle, E. S.; Pople, J. A. *Gaussian 98*, revision A.11.2; Gaussian, Inc.: Pittsburgh, PA, 1998.
(43) http://www.csc.fi/gopenmol/.
(44) Touhara, H.; Okazaki, S.; Okino, F.; Tanaka, H.; Ikari, K.; Nakanishi, K. *J. Chem. Thermodyn*. **1982**, *14*, 145.
(45) Matsumoto, Y.; Touhara, H.; Nakanishi, K.; Watanabe, N. *J. Chem. Thermodyn*. **1977**, *9*, 801.
(46) Ambrosone, L.; D'Errico, G.; Sartorio, R.; Costantino, L. *J. Chem. Soc., Faraday Trans*. **1997**, *93*, 3961.
(47) Samigullin, F. M.; Rodnikova, M. N.; Val'kovskaya, T. M. *Zh. Neorg. Khim.* **1997**, *42*, 1049. (Journal written in Russian.)
(48) Val′kovskaya, T. M.; Rodnikova, M. N.; Samigullin, F. M.; Spivak, G. V. *Zh. Fiz. Khim*. **1998**, *72*, 616. (Journal written in Russian.)
(49) Rodnikova, M. N.; Jastremskij, P. C.; Kharkin, V. S.; Dudnikova, K. T. *Izv. Akad. Nauk. SSSR, Ser. Khim.* **1987**, (N5), 1157. (Journal written in Russian.)
(50) Gubskaya, A. V. Doctoral Thesis, Dalhousie University, Halifax, Nova Scotia, Canada, 2003.
(51) Kusalik, P. G.; Lyubartsev, A. P.; Bergman, D. L.; Laaksonen, A. *J. Phys. Chem. B* **2000**, *104*, 9533.
(52) Hata, T.; Ono, Y. *Chem. Pharm. Bull*. **2000**, *48*, 1660.